Submitted: 12.06.2024.

Accepted: 17.08.2024.

Nanocomposite Cu_xS on Flexible Polymers: Raman Study

Milica Curcic[*1], Martina Gilic[1], Neringa Petrasauskiene[2], Branka Hadzic[1], Jelena Mitric[1], Edita Paluckiene[2]

[1]*Institute of Physics Belgrade, University of Belgrade, Belgrade 11080, Serbia*

[2]*Department of Physical and Inorganic Chemistry, Kaunas University of Technology, LT-50254 Kaunas, Lithuania*

Milica Curcic – ORCID 0000-0001-9239-0912

Martina Gilic – ORCID 0000-0002-5715-7717

Neringa Petrasauskiene – ORCID 0000-0002-8666-112X

Branka Hadzic – ORCID 0000-0001-5459-7461

Jelena Mitric – ORCID 0000-0002-1526-3976

Edita Paluckiene – ORCID 0000-0002-9957-0497

https://doi.org/10.2298/SOS240612034C

Abstract

Flexible polymers modified with copper sulfides have emerged as a novel class of materials, presenting composite structures with remarkable properties suitable for applications in flexible electronics. This study focuses on the deposition of copper sulfide (Cu_xS) layers onto the surfaces of polyamide and polypropylene through the chemical bath deposition method, employing either 2 or 3 deposition cycles. The objective is to explore the impact of deposition cycles and discern the optimal conditions for the deposition process. Comprehensive analysis of the Cu_xS thin films entails techniques such as scanning electron microscopy (SEM), Raman spectroscopy, UV-VIS spectroscopy, and X-ray diffraction to shed light on their structural and optical characteristics.

Keywords: *Copper Sulfide, Nanocomposite, Optical properties, SEM, Raman spectroscopy, UV-VIS spectroscopy, X-ray diffraction*

[*] Corresponding author: Milica Curcic, Institute of Physics Belgrade, University of Belgrade, Pregrevica 118, Belgrade, Serbia
mail: milicap@ipb.ac.rs

1. INTRODUCTION

The CuS, commonly referred to as covellite, demonstrates both superconducting and metallic behaviour at distinct temperatures, as documented in various studies [1-5]. Notably, this material is environmentally friendly and abundant. Its considerable potential for application in Li-ion rechargeable batteries has been widely recognized [6-8]. Additionally, numerous reports highlight its suitability for use in optoelectronic devices [9], solar cells [2, 5, 9, 10], photo catalytic activity [11], chemical sensing [12], and in the fabrication of gas sensors for devices [8, 13, 14]. The origin of superconductivity in CuS is elucidated by its intriguing crystal symmetry. It possesses two distinct crystalline forms at different temperatures. Under ambient conditions, it adopts a hexagonal structure with the space group *P63/mmc* (Z=6) [15, 16, 17]. However, at a low temperature of approximately 55K, it undergoes a structural phase transition from a hexagonal structure to orthorhombic crystal symmetry (*Cmcm*) [17]. Despite extensive investigations of the structure and associated properties of CuS, the findings exhibit mutual inconsistencies. Notably, there are conflicting reports regarding the transition temperatures from the conducting to the superconducting state in CuS. Raveau et al. [18] have documented superconducting behaviour below 40K, while Buckel et al. and Saito et al. independently observed it at remarkably lower temperatures, specifically 1.2K and 1.72K, respectively [19, 20].

Copper sulfide forms five stable phases at room temperature: covellite (CuS), anilite ($Cu_{1.75}S$), digenite ($Cu_{1.8}S$), djurleite ($Cu_{1.95}S$) and chalcocite (Cu_2S) with a crystal structure varying from orthogonal to hexagonal [13]. Copper sulfide films are interesting absorber materials with their film solar cells with ideal optical characteristics [5, 21, 22]. Copper sulfide thin films maintain transmittance in the infrared region, low reflectance in the visible region, and relatively high reflectance in the near infrared region, which has been used in many applications, including solar control coatings, solar energy conversion, electronic, and low-temperature gas sensor applications [14, 21, 22, 23].

Furthermore, disagreement persists regarding the valence state of the Cu atom within the structure. Several oxidation formalisms propose a valence state for the Cu atom ranging from 1 to $1.4e^-$ [20, 24, 25]. Conversely, X-ray absorption spectroscopy (XAS) and X-ray photoelectron spectroscopy (XPS) assert the ionic state of the Cu atom with a valency of $1e^-$ [10, 26, 27]. Kumar et al.'s XAS investigation [28] reports two oxidation states of the Cu atom, corresponding to two distinct crystallographic positions. Moreover, X-ray emission spectroscopy (XES) and X-ray absorption near-edge spectroscopy (XANES) consistently depict the same valence state of the S atom in solid CuS [29, 30, 31]. Consequently, a consensus on the aforementioned aspects of CuS remains elusive.

Nanocomposites are a class of composites wherein at least one of the constituent phases exhibits dimensions within the nanometer range [6]. These materials have emerged as promising alternatives to address the limitations associated with microcomposites and monolithics. However, their preparation presents challenges, particularly in the precise control of elemental composition and stoichiometry

within the nanocluster phase. Widely regarded as materials defining the 21st century, nanocomposites possess distinctive design characteristics and property combinations not observed in traditional composites.

Polymer nanocomposites consist of two primary elements: an organic polymer matrix and inorganic components, often semiconductors. This category encompasses a variety of structures, including three-dimensional metal matrix composites, lamellar composites, colloids, porous materials, gels, and copolymers where nanosized materials are dispersed within the bulk matrix. The properties of these nanocomposites are intricately linked to the characteristics of their components, morphology, and interfaces. To broaden the potential applications of polymer nanocomposites, enhancements in the thermal, mechanical, and electronic properties of conventional polymer materials are essential [32, 33]. This necessitates a concerted effort to improve and optimize these properties, thereby extending the range of possible applications for these advanced materials.

Usage of polymer films, coated with electroconductive layers, has been increasing in the past years due to their elasticity, resistance against corrosion and low toxicity. Electrically conductive Cu_xS layers on polymers can be prepared by methods of vacuum evaporation, activated reactive evaporation [13], electroless deposition [34], successive ionic layer adsorption and reaction (SILAR) [15], chemical bath deposition [35], and sorption–diffusion methods [36, 37].

Polyamide is a semihydrophilic polymer with the ability to absorb ions and molecules from various electrolytes in both aqueous and non-aqueous solutions [38]. This property makes it useful for a range of applications. Polyamide is known for its high thermal resistance and excellent mechanical properties. Types of Polyamide:

- Nylon 6 (PA 6): This is a widely used polyamide with good mechanical properties and excellent resistance to abrasion.
- Nylon 66 (PA 66): Known for its high melting point and chemical resistance, it is commonly used in the automotive industry.

Nylon is widely used in the textile industry for the production of fabrics, garments, and carpets. Polyamide is used in various automotive components, such as gears, bushings, and engine parts. Nylon is used in the production of durable and heat-resistant plastic parts.

On the other hand, polypropylene (PP) is an economical thermoplastic polymer that boasts outstanding chemical, physical, and mechanical characteristics. These include flame resistance, transparency, a high heat distortion temperature, dimensional stability, and recyclability, making it well-suited for a wide array of applications [39, 40, 41, 42]. Polypropylene is relatively rigid, has a high melting point (160–166 °C), low density (0.91–0.94 g/cm^3), and demonstrates good resistance to high temperatures, chemical agents, and impacts [43].

This study aimed to investigate the morphology and optical properties of copper sulfide layers formed on polyamide and polypropylene film using the chemical bath deposition method. Structural characterization of the thin films was performed with the help of X-ray diffraction, and Scanning

Electron Microscopy, while the optical properties were characterized with UV/VIS spectroscopy and Raman spectroscopy.

2. MATERIALS AND METHODS

2.1. Thin films formation

Commercially available PA (PA 6, Tecamid 6, Ensinger GmbH (Germany) and PP (Proline X998, KWH Plast, Finland) films were chosen as flexible substrates for the deposition of thin films of copper sulfide Cu_xS). The nominal characteristics of PP and PA films provided by the manufacturer are given in Table 1.

TABLE 1. Characteristics of PA and PP films

Polymer	Appearance	Thickness (μm)	Density (g/cm^3)	Surface Resistance (Ω)
PA	opaque	500	1.13	10^{12}
PP	clear	150	0.90	10^{16}

Acetone (CH_3COCH_3, 99.5%), alcohol (CH_3CH_2OH, 95%), and all other chemicals used for deposition were purchased from Sigma-Aldrich and were of analytical grade, used without further purification.

Before the experiments, the PA films were boiled in distilled water for 2 h to remove the remaining un-polymerized monomer residues. PP films were etched for 25 min at 90 °C with oxidizing solution (H_2SO_4/H_3PO_4 (1:1), saturated with CrO_3) [39] Then, samples of polymers were dried with filter paper and incubated over anhydrous $CaCl_2$ for 24 h.

The Cu_xS thin films deposit was carried out at room temperature by using the following procedure: 0.05 M $CuCl_2$ and 0.05 M $Na_2S_2O_3$ were mixed, and the pH of the resultant solution was adjusted to 3. The pre-treated PA and PP samples were vertically immersed along the wall of the reactor and were left undisturbed for the deposition of Cu_xS films for 16 h at 20 °C. At the end of the deposition time, the samples were taken out and then the substrate was rinsing with distilled water for 30 s to remove the desorbed ions and dried in a desiccator for 8 h. The deposition process was carried out by repeating such deposition cycles 3 times. The formed samples were annealed at 80 ºC for 30 minutes in an air atmosphere.

2.2. Thin films characterisation

Structural characterization of polymers coated with films was done by a Scanning Electron Microscope Hitachi SU8030 supported with a secondary electron detector.

Raman measurements were carried out in a backscattering configuration on a Horiba XploRA confocal Raman instrument equipped with a charge-coupled-device (CCD) detector. The spectra acquisition was carried out using an excitation laser wavelength of 532 nm of ca. 100mW power, in a spectral range of 200 – 1100 cm^{-1}.

The UV/VIS diffusion reflectance spectra were recorded in the wavelength range of 300 – 1000 nm on a Shimadzu UV-2600 spectrophotometer equipped with an integrated sphere. The absorbance spectra were measured relative to a reference sample of virgin polymers (PA and PP). The optical band gap from the absorbance measurements was calculated using the Tauc plot.

X-ray diffraction (XRD) measurements were performed using a Philips PW 1050 diffractometer equipped with a PW 1730 generator, 40 kV × 20 mA, using Ni filtered Co Kα radiation of 0.1778897 nm at room temperature. Measurements were carried out in the 2 h range of 10 to 90° with a scanning step of 0.05° and a scan time of 10 s per step.

3. RESULTS AND DISCUSSION

3.1. Scanning Electron Microscopy

The scanning electron microscopy technique was used to evaluate the changes in the surface morphology of polyamide and polypropylene after 2 or 3 cycles of copper sulfide Cu_xS thin films deposition. The description makes reference to SEM micrographs in Figure 1. In Figure 1(a), the SEM images illustrate the initial state of the polymers, with PA on the left and PP on the right. In Figure 1(b), the SEM images indicate that copper sulfide grains exhibit irregular shapes and varying sizes after 2 cycles of film deposition. Following 3 cycles of film deposition, Figure 1(c) reveals micrographs displaying a dense structure composed of a single type of small, closely packed microcrystals. The thin copper sulfide films on the surfaces of PP and PA are well-dispersed, relatively uniform, and consist of randomly oriented particles. Such morphological characteristics can result in a highly rough surface with significant porosity, potentially leading to increased catalytic activity. The pronounced agglomeration on the surface of thin films indicates semiconductor characteristics of Cu_xS.

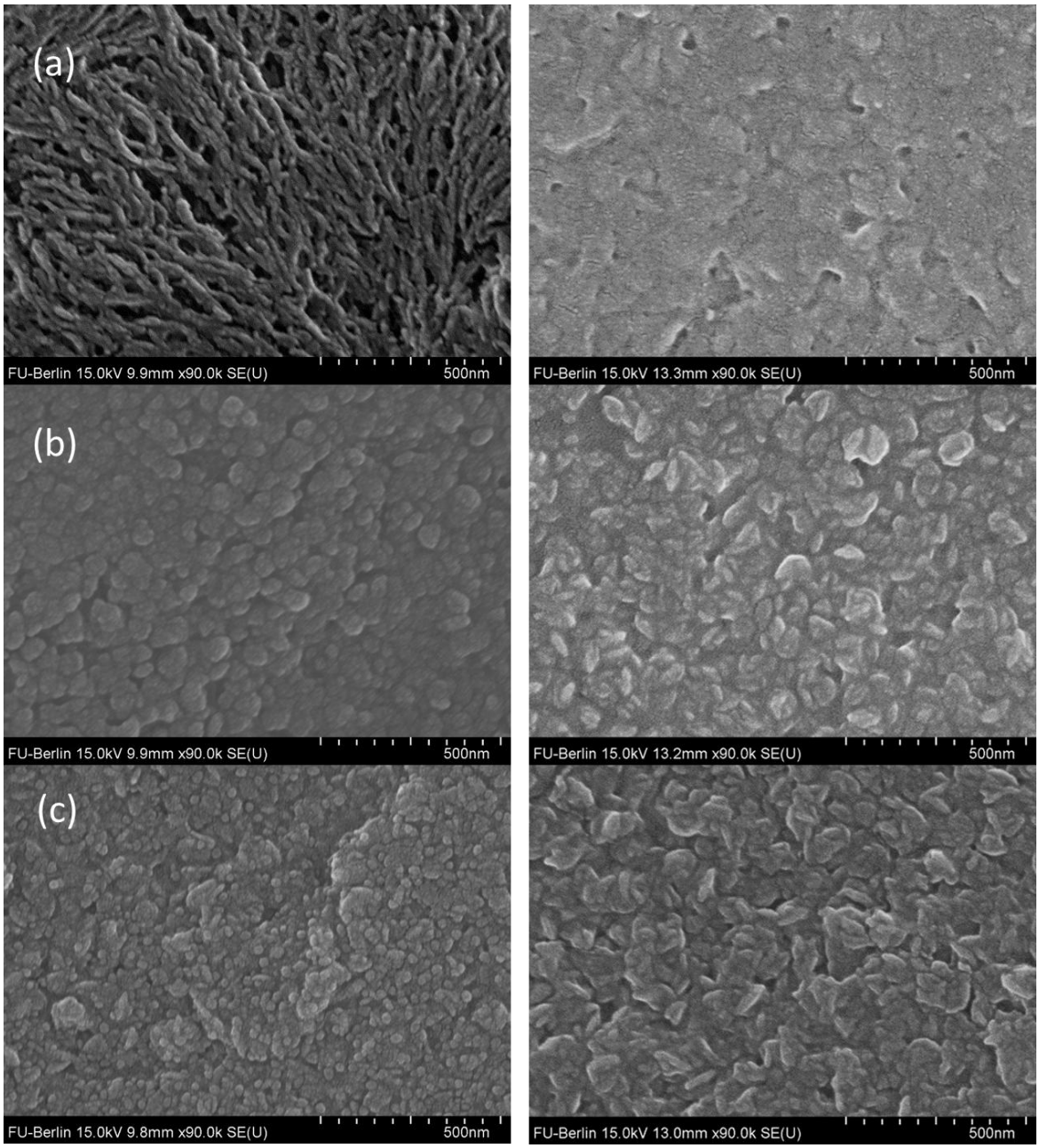

Figure 1. SEM micrographs of PA (left) and PP (right) polymers: (a) virgin polymers, (b) after 2 cycles of film deposition, and (c) after 3 cycles of film deposition.

PA showcases a porous structure reminiscent of seaweed, indicating a high degree of porosity. Consequently, it necessitates 3 cycles of film deposition to achieve the desired results. The substantial porosity on the surface of PA promotes strong adhesion and facilitates the growth of the copper sulfide film. In contrast, the surface of PP bears a resemblance to melted plastic and displays a porosity relatively lower than that of PA. For PP, the optimal outcome is achieved with 2 cycles of film deposition, as further cycles result in the agglomeration of film material.

These findings underscore the importance of customizing the number of film deposition cycles to align with the specific surface characteristics of different polymers. The choice of cycle count plays a pivotal role in shaping the resulting film morphology and its associated properties.

3.2. X-ray diffraction

The crystallinity and the preferred crystal orientation of the Cu_xS nanocomposite were analyzed by the XRD method. Figure 2 shows the diffraction pattern of the film. There is one high intensity diffraction peak around at 2θ=28,46° which is related to lattice planes of (101) (PDF 06-0464) the hexagonal phase of the Cu_xS covellite structure [4, 6, 22, 39]. The other peak that appeared with lower intensities around at 2θ=47° is related to the lattice planes of (107) the Cu_xS covellite structure [39].

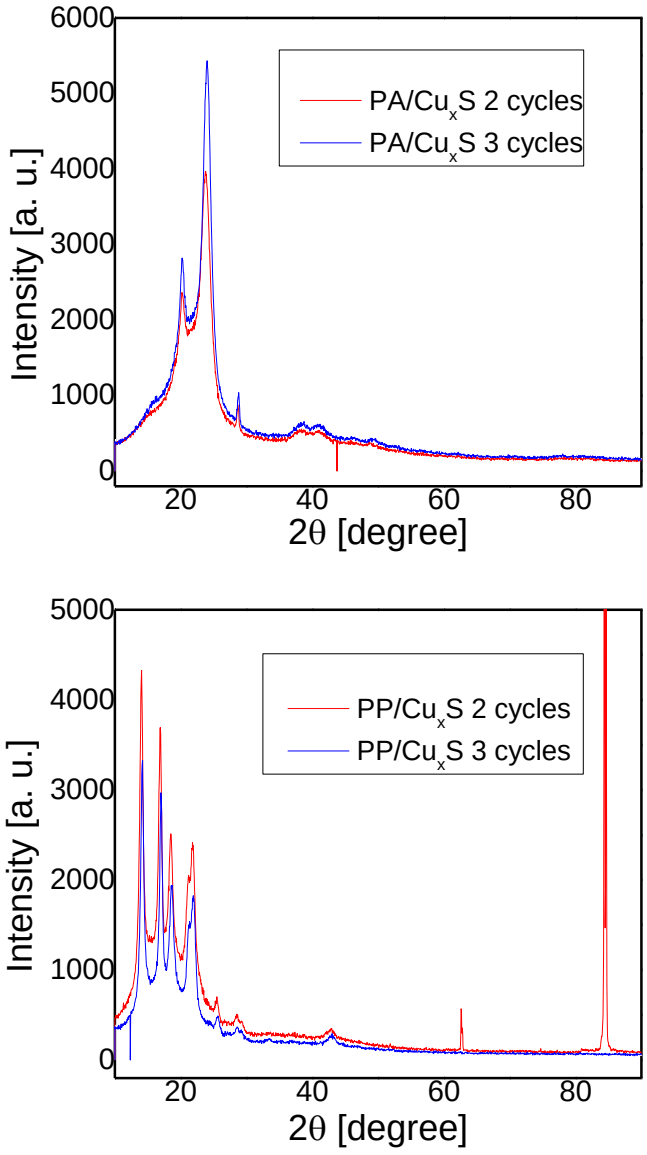

Figure 2. X-ray diffraction results of PA/Cu_xS and PP/Cu_xS after 2 or 3 cycles of deposition.

The peak of lower intensity in our case is visible only in the instance of Cu_xS on the flexible polymer PA. We also observe the appearance of an additional peak of very low intensity, noticeable only in the case of PP/Cu_xS after 3 cycles, corresponding to 2θ=32.49 degrees. This pertains to the $Cu_{2-x}S$ ($0.6 \leq x \leq 1$) phase, present in the sample at a significantly lower concentration, as confirmed by the Raman spectrum [38].

3.3. UV-VIS Spectroscopy

UV/VIS analysis is able to describe the electrical properties of the materials. Bandgap (E_g), which indicated conductivity of the material: conductor, semiconductor or insulator, can be calculated from the data of this investigation. The optical absorption data have been analyzed to determine the optical bandgap values using the Tauc's relation [44]:

$$\alpha h = A\left(h\nu - E_g\right)^n \quad (1)$$

where α – the absorption coefficient, hν – the photon energy, *A* – the proportionality constant, E_g – the optical bandgap, n – a constant associated with different types of electronic transitions.

The absorbance spectra of the film were measured in the range of 200–1000 nm, as shown in Figure 4. Films have max absorbance around 300 nm and then absorbance drops, one more hill in NIR region, around 900 nm, indicates a copper-deficient compound (Cu_xS or less).

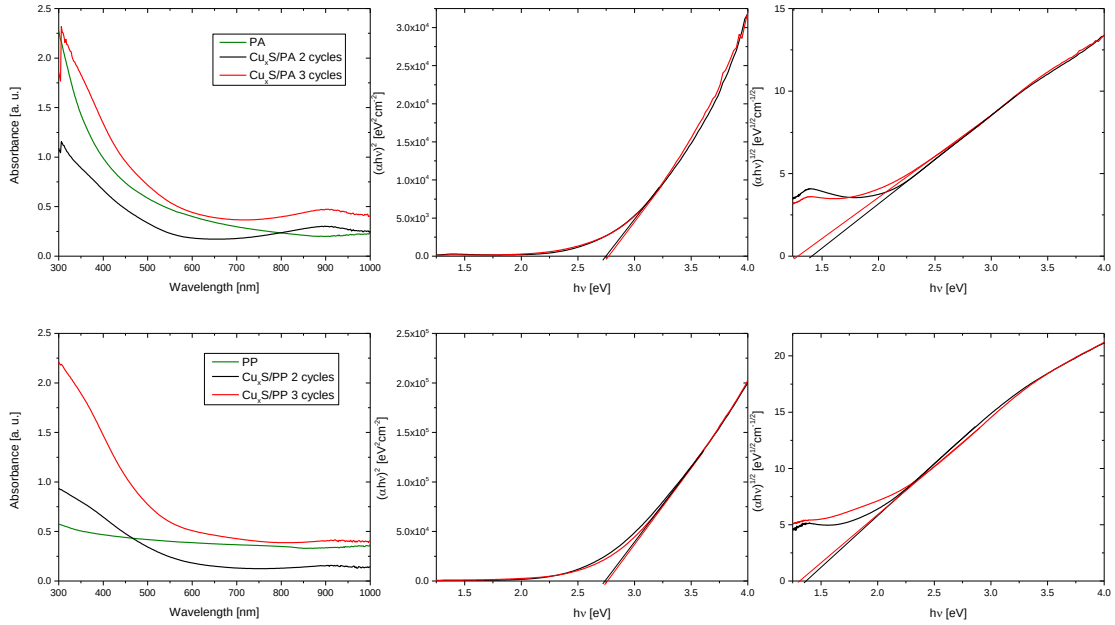

Figure 3. UV-VIS Absorbance spectra and spectra plot of $(\alpha h\nu)^2$ or$(\alpha h\nu)^{1/2}$ versus Photon energy (hν) for polymers with thin films.

The experimental values of $(\alpha h\nu)^2$ against hν are plotted in Figure 3. The variation of $(\alpha h\nu)^2$ with hν is linear, indicating that a direct transition is present. Extrapolating the straight-line portion of the plot of $(\alpha h\nu)^2$ against hν to energy axis for the zero-absorption coefficient gives the optical band gap energy of the samples.

The energy band gap values for a thin film using PA polymer, which has a thickness of 0.05 cm, are as follows:

For the direct band gap:

- After 2 cycles: 2.75 eV
- After 3 cycles: 2.78 eV

For the indirect band gap:

- After 2 cycles: 1.41 eV
- After 3 cycles: 1.29 eV

These values represent the amount of energy required to transition an electron from the valence band to the conduction band. The direct band gap signifies the energy difference between the highest energy state in the valence band and the lowest energy state in the conduction band, whereas the indirect band gap considers transitions involving changes in momentum.

It is important to note that the number of film deposition cycles can have a discernible impact on the band gap values. In this particular case, subtle variations in the band gap values are observed between 2 and 3 cycles of film deposition for both direct and indirect transitions.

The energy band gap values for a thin film using PP (polypropylene) polymer, with a thickness of 0.02 cm, are as follows:

For the direct band gap:

- After 2 cycles: 2.76 eV
- After 3 cycles: 2.77 eV

For the indirect band gap:

- After 2 cycles: 1.37 eV
- After 3 cycles: 1.31 eV

It is noteworthy that the values of the direct band gap slightly exceed the typical range reported in the literature, which generally falls within 2.5 eV [45]. Although the film thickness did not differ significantly, the direct band gap values for all four samples were remarkably consistent. These results underscore that the PP/Cu_xS and PA/Cu_xS composites exhibit clear semiconductor properties, and their direct band gap values suggest their suitability as promising materials for the fabrication of solar cells.

3.4. Raman Spectroscopy PA and PP polymers with thin films

Raman spectroscopy provides valuable insights into the local structure of materials. Based on the XRD patterns, Cu_xS and $Cu_{2-x}S$ can be expected in the Raman spectra. The knowledge of the vibrational properties of bulk material is deciding for the analysis of the vibration properties of nanoparticles; hence, we began the analysis of vibrational properties with a brief report of the data from the literature, which are related to the registered phases. Copper sulfide exists in five stable phases at room temperature. These phases have crystal structures that range from orthogonal to hexagonal. Hexagonal CuS crystals have a space group D_{6h}^4 and a primitive unit cell that contains 12 atoms, namely, six of Cu and six S ones. Group theory analysis predicts eight Raman active modes of the zone-center for this crystal [46]:

$$2A_{1g} + 2E_{1g} + 4E_{2g} \quad (2)$$

The Raman spectra are usually analyzed using the convolution of the Lorentzian functions, where each line has intensity (I), given with:

$$I(\omega) = \frac{2A}{\pi} \frac{W}{4(w-w_c)^2+W^2} \quad (3)$$

where ω_c, W, and A are the position of the maximum, the half-width of the peak, and the peak intensity, respectively. In Figure 4, Raman spectra are depicted for PA and PP polymers with thin Cu_xS films following 2 or 3 cycles of film deposition, spanning the frequency range of 200-1100 cm^{-1}.

The data measured depicted with lines in Figure 4 resemble the calculated thick curve, which represents the sum of the components each one defined with Equation 3.

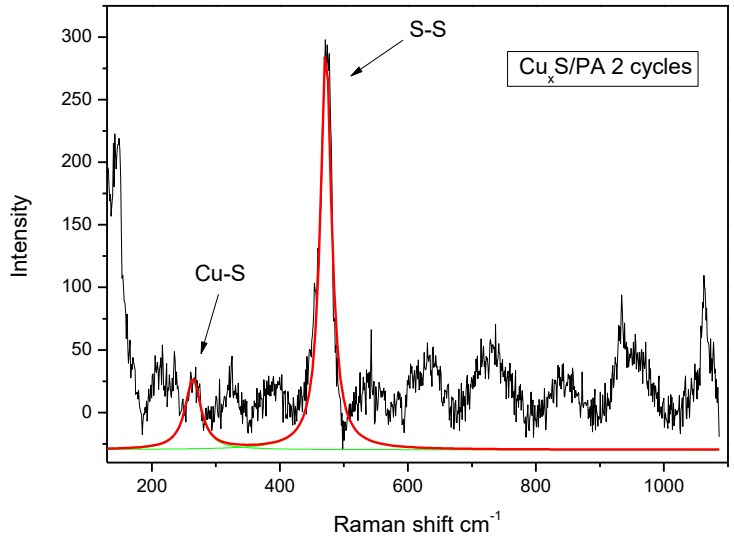

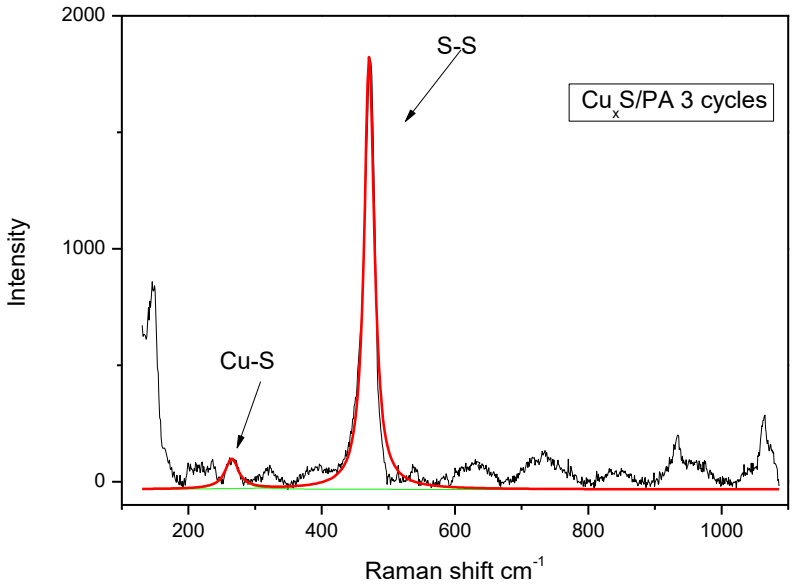

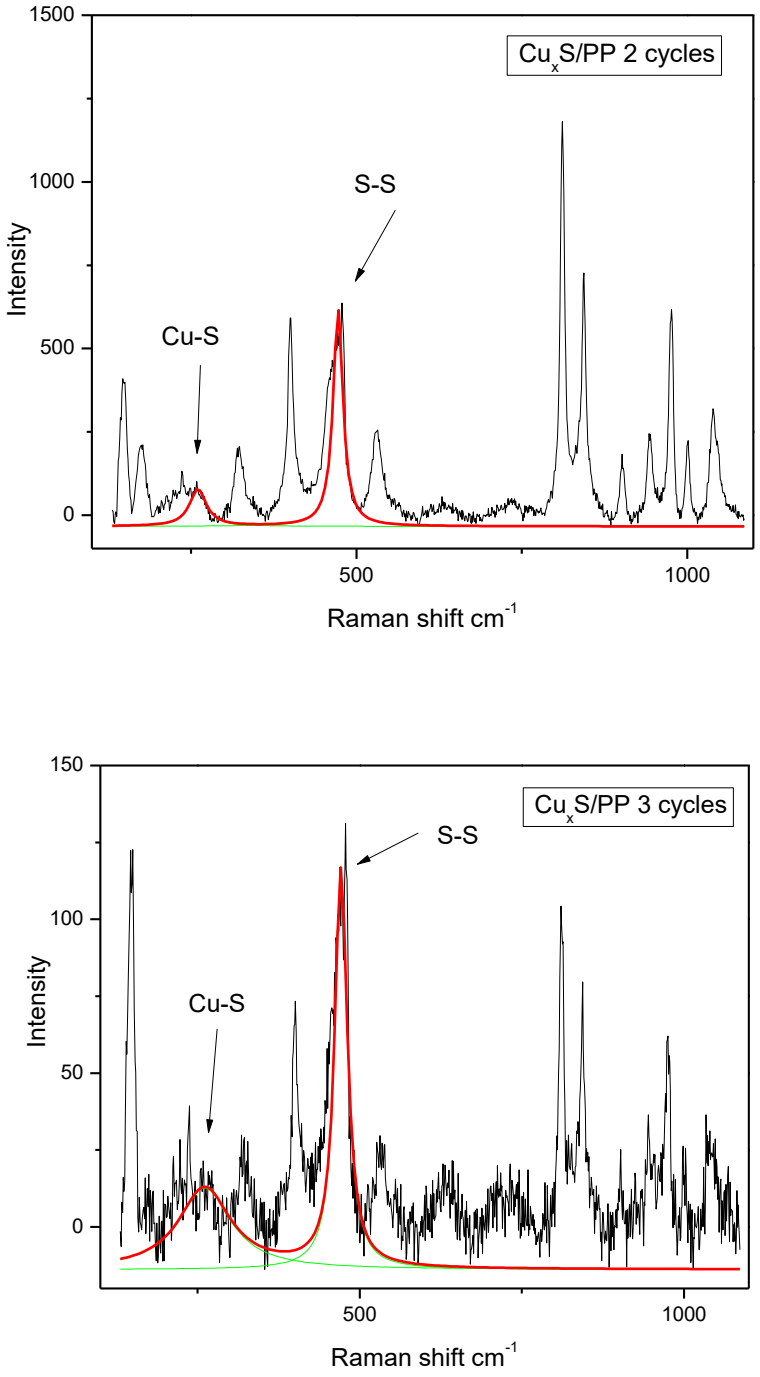

Figure 4. Raman spectra of the Cu_xS nanocomposite on PP and PA polymers.

A small peak at 265 cm^{-1} corresponds to the Cu-S vibration in covellite (Cu_xS) [46]. Additionally, a highly sharp peak at 471 cm^{-1} is attributed to the S-S stretching vibration of S_2 ions at the 4e sites [46]. The dominance of the S-S stretch band in the spectrum, particularly when the potential enters the region where $Cu_{2-x}S$ is formed [47], suggests that lattice atoms are well-ordered in a periodic array. This result underscores the capability of Raman spectroscopy to distinguish between

copper sulfides with and without S-S bonding. Notably, the intensity of this peak increases after 3 cycles of film deposition. By increasing the number of deposition cycles, stable $Cu_{2-x}S$ phases are obtained, opening up possibilities for new applications.

Raman spectroscopy is a technique that has enabled the determination of Cu_xS and $Cu_{2-x}S$ phases composition in thin films nanocomposite. The presence of the Cu_xS phase is approximately 2,5%, while the $Cu_{2-x}S$ phase is three times higher. In the case of PA polymer, after the third cycle of deposition, there is an increased agglomeration indicated by increased intensity of the mode. In the case of nanocomposite with PP, there is no pronounced agglomeration.

CONCLUSION

Copper sulfide thin films are deposited on a flexible polymer substrate using the chemical bath deposition method. Scanning electron microscopy was used to evaluate the changes in surface morphology of PA and PP after 2 or 3 cycles of film deposition Cu_xS. The thin copper sulfide films on surface of PP and PA are well dispersed, relatively uniform, and consist of randomly oriented particles. The XRD method was used to analyze the crystallinity and preferred crystal orientation of Cu_xS nanocomposite. There is one high intensity diffraction peak around at $2\theta=28,46°$ which is related to lattice planes of (101) the hexagonal phase of the Cu_xS covellite structure. The other peak appeared with lower intensities around at $2\theta=47°$ is related to the lattice planes of (107) the Cu_xS covellite structure. The peak of lower intensity in our case is visible only in the instance of Cu_xS on the flexible polymer PA. We also observe the appearance of an additional peak of very low intensity, noticeable only in the case of PP/Cu_xS after 3 cycles, corresponding to $2\theta=32.49$ degrees. This pertains to the $Cu_{2-x}S$ ($0.6\leq x\leq 1$) phase, present in the sample at a significantly lower concentration, as confirmed by the Raman spectrum. Direct and indirect allowed transitions are exhibited for Cu_xS thin films with energy band gaps of 2.75–2.78 eV and 1.29–1.41 eV, respectively. Direct band gap values exceeding the conventional literature range indicate that these composites possess desirable semiconductor characteristics, rendering them potentially excellent candidates for utilization in photovoltaics applications. Raman spectroscopy has been utilized to analyze composition of Cu_xS and $Cu_{2-x}S$ phases in thin film nanocompostion. In Raman spectra small peak at $265cm^{-1}$ corresponds to the Cu-S vibration in covellite (Cu_xS). Highly sharp peak at 471 cm^{-1} is attributed to the S-S stretching vibration of S_2 ions at the $4e^-$ sites. The dominance of the S-S stretch band in the spectrum, particularly when the potential enters the region where $Cu_{2-x}S$ is formed, suggests that lattice atoms are well-ordered in a periodic array.

Acknowledgement

This research was supported by the Science Fund of the Republic of Serbia, Grant No. 7504386, Nano Object in Own Matrix-Self Composite (NOOM-SeC).

References:

1. Rezig, B.; Duchemin, S.; Guastavino, F. Evaporated Layers of Cuprous Sulfides: Technology and Methods of Characterization. *Solar Energy Materials* **1979**, *2*, 53. https://doi.org/10.1016/0165-1633(79)90030-3

2. Yepsen, O.; Yáñez, J.; Mansilla, H.D. Photocorrosion of Copper Sulfides: Toward a Solar Mining Industry. *Solar Energy* **2018**, *171*, 106. https://doi.org/10.1016/j.solener.2018.06.049

3. Lenggoro, I.W.; Kang, Y.C.; Komiya, T.; Okuyama, K.; Tohge, N. Formation of Submicron Copper Sulfide Particles Using Spray Pyrolysis Method. *Japanese Journal of Applied Physics, Part 2: Letters* **1998**, *37*, L288. https://iopscience.iop.org/article/10.1143/JJAP.37.L288/pdf

4. Sabah, F.A.; Ahmed, N.M.; Hassan, Z.; Rasheed, H.S. High Performance CuS p-Type Thin Film as a Hydrogen Gas Sensor. *Sens Actuators A Phys* **2016**, *249*, 68. http://dx.doi.org/10.1016/j.snb.2017.03.020

5. Wu, C.; Zhang, Z.; Wu, Y.; Lv, P.; Nie, B.; Luo, L.; Wang, L.; Hu, J.; Jie, J. Flexible CuS Nanotubes–ITO Film Schottky Junction Solar Cells with Enhanced Light Harvesting by Using an Ag Mirror. *Nanotechnology* **2013**, *24*, 045402. https://iopscience.iop.org/article/10.1088/0957-4484/24/4/045402

6. Zhang, Y.; Tian, J.; Li, H.; Wang, L.; Qin, X.; Asiri, A.M.; Al-Youbi, A.O.; Sun, X. Biomolecule-Assisted, Environmentally Friendly, One-Pot Synthesis of CuS/Reduced Graphene Oxide Nanocomposites with Enhanced Photocatalytic Performance. *Langmuir* **2012**, *28*, 12893. https://doi.org/10.1021/la303049w

7. Peng, H.; Ma, G.; Sun, K.; Mu, J.; Wang, H.; Lei, Z. High-Performance Supercapacitor Based on Multi-Structural CuS@polypyrrole Composites Prepared by in Situ Oxidative Polymerization. : *J. Mater. Chem. A* **2014**, *2*, 3303. https://doi.org/10.1039/C3TA13859C

8. Xu, J.; Zhang, J.; Yao, C.; Dong, H. Synthesis of Novel Highly Porous CuS Golf Balls by Hydrothermal Method and their Application in Ammonia Gas Sensing. *Journal of the Chilean Chemical Society* **2013**, *58*, 1722. http://dx.doi.org/10.4067/S0717-97072013000200017

9. Froment, M.; Cachet, H.; Essaaidi, H.; Maurin, G.; Cortes, R. Metal Chalcogenide Semiconductors Growth from Aqueous Solutions. *Pure and Applied Chemistry* **1997**, *69*, 77. https://doi.org/10.1351/pac199769010077

10. Pattrick, R.A.D.; Mosselmans, J.F.W.; Charnock, J.M.; England, K.E.R.; Helz, G.R.; Garner, C.D.; Vaughan, D.J. The Structure of Amorphous Copper Sulfide Precipitates: An X-Ray Absorption Study. *Geochim Cosmochim Acta* **1997**, *61*, 2023. https://doi.org/10.1016/S0016-7037(97)00061-6

11. Flores-García, E.; González-García, P.; González-Hernández, J.; Ramírez-Bon, R. Non-Toxic Growth of Cu_xS Thin Films in Alkaline Medium by Ammonia Free Chemical Bath Deposition. *Optik (Stuttg)* **2017**, *145*, 589. https://doi.org/10.1016/j.ijleo.2017.08.043

12. Kozhevnikova, N.S.; Maskaeva, L.N.; Markov, V.P.; Lipina, O.A.; Chufarov, A.U.; Kuznetsov, M. V. One-Pot Green Synthesis of Copper Sulfide (I) Thin Films with p-Type Conductivity. *Mater Chem Phys* **2020**, *242*, 122447. https://doi.org/10.1016/j.matchemphys.2019.122447

13. Grozdanov, I.; Najdoski, M. Optical and Electrical Properties of Copper Sulfide Films of Variable Composition. *J Solid State Chem* **1995**, *114*, 469. https://doi.org/10.1006/jssc.1995.1070

14. Galdikas, A.; Mironas, A.; Strazdiene, V.; Setkus, A.; Ancutiene, I.; Janickis, V. Room-Temperature-Functioning Ammonia Sensor Based on Solid-State CuxS Films. *Sens Actuators B Chem* **2000**, *67*, 76. https://doi.org/10.1016/S0925-4005(00)00408-1

15. Pathan, H.M.; Desai, J.D.; Lokhande, C.D. Modified Chemical Deposition and Physico-Chemical Properties of Copper Sulphide (Cu_2S) Thin Films. *Appl Surf Sci* **2002**, *202*, 47. https://doi.org/10.1016/S0169-4332(02)00843-7

16. Arora, S.; Kabra, K.; Joshi, K.B.; Sharma, B.K.; Sharma, G. Structural, Elastic, Thermodynamic and Electronic Properties of Covellite, CuS. *Physica B Condens Matter* **2020**, *582*, 311142. https://doi.org/10.1016/j.physb.2018.11.007

17. Fjellvag, H.; Gronvold, F.; Stolen, S.; Andresen, A.F.; Muller-Kafer, R.; Simon, A. Low-Temperature Structural Distortion in CuS. *Zeitschrift fur Kristallographie - New Crystal Structures* **1988**, *184*, 111. https://doi.org/10.1524/zkri.1988.184.1-2.111

18. Raveau, B.; Sarkar, T. Superconducting-like Behaviour of the Layered Chalcogenides CuS and CuSe below 40 K. *Solid State Sci* **2011**, *13*, 1874. https://doi.org/10.1016/j.solidstatesciences.2011.07.022

19. Buckel, W.; Hilsch, R. Zur Supraleitung von Kupfersulfid. *Zeitschrift für Physik* **1950**, *128*, 324. https://doi.org/10.1007/BF01333079

20. Saito, S.-H.; Kishi, H.; Nié, K.; Nakamaru, H.; Wagatsuma, F.; Shinohara, T. Cu NMR Studies of Copper Sulfide. *Phys. Rev. B* **1997**, *55*, 14527. https://journals.aps.org/prb/pdf/10.1103/PhysRevB.55.14527

21. Hamed, M.S.G.; Mola, G.T. Copper Sulphide as a Mechanism to Improve Energy Harvesting in Thin Film Solar Cells. *J Alloys Compd* **2019**, *802*, 252. https://doi.org/10.1016/j.jallcom.2019.06.108

22. Marimuthu, T.; Anandhan, N.; Panneerselvam, R.; Ganesan, K.P.; Roselin, A.A. Synthesis and Characterization of Copper Sulfide Thin Films for Quantum Dot Sensitized Solar Cell and Supercapacitor Applications. *Nano-Structures & Nano-Objects* **2019**, *17*, 138. https://doi.org/10.1016/j.nanoso.2018.12.004

23. Sangamesha, M.A.; Pushpalatha, K.; Shekar, G.L.; Shamsundar, S. Preparation and Characterization of Nanocrystalline CuS Thin Films for Dye-Sensitized Solar Cells. *ISRN Nanomater* **2013**, 1. https://doi.org/10.1155/2013/829430

24. Gainov, R.R.; Dooglav, A. V; Pen'kov, I.N.; Mukhamedshin, I.R.; Mozgova, N.N.; Evlampiev, I.A.; Bryzgalov, I.A. Phase Transition and Anomalous Electronic Behavior in the Layered Superconductor CuS Probed by NQR. *Phys. Rev. B* **2009,** *79*, 075115. https://doi.org/10.1103/PhysRevB.79.075115

25. Mazin, I.I. Structural and Electronic Properties of the Two-Dimensional Superconductor CuS with 113-Valent Copper. *Phys Rev B Condens Matter Mater Phys* **2012**, *85*, 115133. https://doi.org/10.1103/PhysRevB.85.115133

26. Wei Goh, S.; Buckley, A.N.; Lamb, R.N.; Rosenberg, R.A.; Moran, D. The Oxidation States of Copper and Iron in Mineral Sulfides, and the Oxides Formed on Initial Exposure of Chalcopyrite and Bornite to Air. *Geochimica et Cosmochimica Acta* **2006,** *70*, 2210. https://doi.org/10.1016/j.gca.2006.02.007

27. Van der Laan, G.; Pattrick, R.A.D.; Henderson, C.M.B.; Vaughan, D.J. Oxidation State Variations in Copper Minerals Studied with Cu 2p X-Ray Absorption Spectroscopy. *Journal of Physics and Chemistry of Solids* **1992**, *53*, 1185. https://doi.org/10.1016/0022-3697(92)90037-E

28. Kumar, P.; Nagarajan, R.; Sarangi, R. Quantitative X-Ray Absorption and Emission Spectroscopies: Electronic Structure Elucidation of Cu2S and CuS. *J Mater Chem C Mater* **2013**, *1*, 2448. https://doi.org/10.1039/C3TC00639E

29. Nakai, I.; Sugitani, Y.; Nagashima, K.; Niwa, Y. X-Ray Photoelectron Spectroscopic Study of Copper Minerals. *Journal of Inorganic and Nuclear Chemistry* **1978**, *40*, 789. https://doi.org/10.1016/0022-1902(78)80152-3

30. Kurmaev, E.Z.; Van Ek, J.; Ederer, D.L.; Zhou, L.; Callcott, T.A.; Perera, R.C.C.; Cherkashenko, V.M.; Shamin, S.N.; Trofimova, V.A.; Bartkowski, S.; et al. Experimental and Theoretical Investigation of the Electronic Structure of Transition Metal Sulphides: CuS, And. *Journal of Physics: Condensed Matter* **1998**, *10*, 1687. https://doi.org/10.1088/0953-8984/10/7/016

31. Li, D.; Bancroft, G.M.; Kasrai, M.; Fleet, M.E.; Feng, X.H.; Yang, B.X.; Tan, K.H. S K- and L-Edge XANES and Electronic Structure of Some Copper Sulfide Minerals. *Phys Chem Miner* **1994**, *21*, 317. https://doi.org/10.1007/BF00202096

32. Fu, S.; Sun, Z.; Huang, P.; Li, Y.; Hu, N. Some Basic Aspects of Polymer Nanocomposites: A Critical Review. *NMS* **2019,** *1*, 2. https://doi.org/10.1016/j.nanoms.2019.02.006

33. Khan, I.; Khan, I.; Saeed, K.; Ali, N.; Zada, N.; Khan, A.; Ali, F.; Bilal, M.; Akhter, M.S. Polymer Nanocomposites: An Overview. *Smart Polymer Nanocomposites* **2023,** 167. https://doi.org/10.1016/B978-0-323-91611-0.00017-7

34. Chen, Y.-H.; Huang, C.-Y.; Lai, F.-D.; Roan, M.-L.; Chen, K.-N.; Yeh, J.-T. Electroless Deposition of the Copper Sulfide Coating on Polyacrylonitrile with a Chelating Agent of Triethanolamine and Its EMI Shielding Effectiveness. *Thin Solid Films* **2009**, *517*, 4984. https://doi.org/10.1016/j.tsf.2009.03.137

35. Pathan, H.M.; Desai, J.D.; Lokhande, C.D. Modified Chemical Deposition and Physico-Chemical Properties of Copper Sulphide (Cu 2 S) Thin Films. *Appl Surf Sci* **2002**, *202*, 47. https://doi.org/10.1016/S0169-4332(02)00843-7

36. Balciunaite, E.; Petrasauskiene, N.; Alaburdaite, R.; Jakubauskas, G.; Paluckiene, E. Formation and Properties of Mixed Copper Sulfide (Cu_xS) Layers on Polypropylene. *Surfaces and Interfaces* **2020**, *21*, 100801. https://doi.org/10.1016/j.surfin.2020.10080

37. Petrasauskiene, N.; Paluckiene, E.; Alaburdaite, R.; Gilić, M. Deposition of Copper Sulfide Films on Polyamide Surface. *Science of Sintering* **2022**, *54*, 139. https://doi.org/10.2298/SOS2202139P

38. Janickis, V.; Petrašauskiene, N.; Žalenkiene, S.; Morkvenaite-Vilkoňciene, I.; Ramanavĭcius, A. Morphology of CdSe-Based Coatings Formed on Polyamide Substrate. *J Nanosci Nanotechnol* **2018**, *18*, 604. https://doi.org/10.1166/jnn.2018.13927

39. Alaburdaite, R.; Paluckiene, E. Investigation of Cu_xS Layers on Polypropylene Film Formed by Using Different Sulfuring Agents. *Chalcogenide Letters* **2018**, *15*, 139. https://www.chalcogen.ro/139_AlaburdaiteR.pdf

40. Noeske, M.; Degenhardt, J.; Strudthoff, S.; Lommatzsch, U. Plasma Jet Treatment of Five Polymers at Atmospheric Pressure: Surface Modifications and the Relevance for Adhesion. *Int J Adhes Adhes* **2004**, *24*, 171. https://doi.org/10.1016/j.ijadhadh.2003.09.006

41. Moloney, M.G. Functionalized Polymers by Chemical Surface Modification. *J. Phys. D: Appl. Phys* **2008**, *41*, 9. http://dx.doi.org/10.1088/0022-3727/41/17/174006

42. Choi, Y.H.; Kim, J.H.; Paek, K.H.; Ju, W.T.; Hwang, Y.S. Characteristics of Atmospheric Pressure N2 Cold Plasma Torch Using 60-Hz AC Power and Its Application to Polymer Surface Modification. *Surf Coat Technol* **2005**, *193*, 319. https://doi.org/10.1016/j.surfcoat.2004.08.145

43. Alaburdaitė, R.; Krylova, V. Study of Thermo-Oxidative Chemical Pre-Treatment of Isotactic Polypropylene. *J Therm Anal Calorim* **2014**, *118*, 1331. https://doi.org/10.1007/s10973-014-4226-0

44. Tauc, J.; Grigorovici, R.; Vancu, A. Optical Properties and Electronic Structure of Amorphous Germanium. *Physica status solidi (b)* **1966**, *15*, 627. https://doi.org/10.1002/pssb.19660150224

45. Naşcu, C.; Pop, I.; Popescu, V.; Indrea, E.; Bratu, I. Spray Pyrolysis Deposition of CuS Thin Films. *Mater Lett* **1997**, *32*, 73. https://doi.org/10.1016/S0167-577X(97)00015-3

46. Ishii, M.; Shibata, K.; Nozaki, H. Anion Distributions and Phase Transitions in $CuS_{1-X}Se_x$(x = 0-1) Studied by Raman Spectroscopy. *J Solid State Chem* **1993**, *105*, 504. https://doi.org/10.1006/jssc.1993.1242.

47. Trajic, J.; Curcic, M.; Casas Luna, M.; Romcevic, M.; Remesova, M.; Matej Balaz,|; Ladislav Celko, |; Dvorak, K.; Romcevic, N. Vibrational Properties of the Mechanochemically Synthesized Cu_2SnS_3 : Raman Study. *J. Raman Spectrosc* **2022**, *53*, 977. https://doi.org/10.1002/jrs.6318

Апстракт

Флексибилни полимери модификовани бакар-сулфидима појавили су се као нова класа материјала, представљајући композитне структуре са изванредним особинама погодним за примену у флексибилној електроници. Ова студија се фокусира на депоновање слојева бакар-сулфида (Cu_xS) на површине полиамида и полипропилена путем методе хемијског таложења из купке, применом 2 или 3 циклуса таложења. Циљ је истражити утицај броја циклуса таложења и утврдити оптималне услове за процес таложења. Свеобухватна анализа танких филмова Cu_xS обухвата технике као што су скенирајућа електронска микроскопија (SEM), Раман спектроскопија, UV-VIS спектроскопија и рендгенска дифракција како би се расветлиле њихове структурне и оптичке карактеристике.

***Кључне речи**: Бакар-сулфид, Нанокомпозит, Оптичка својства, SEM, Раман спектроскопија, UV-VIS спектроскопија, Рендгенска дифракција*